THE ASTROPHYSICAL JOURNAL, 474:L61–L64, 1997 January 1
© 1997. The American Astronomical Society. All rights reserved. Printed in U.S.A.

MAGNETIC RECONNECTION COUPLED WITH HEAT CONDUCTION

TAKAAKI YOKOYAMA AND KAZUNARI SHIBATA
National Astronomical Observatory, Mitaka, Tokyo, 181 Japan; yokoyama@solar.mtk.nao.ac.jp
Received 1996 August 30; accepted 1996 October 7

ABSTRACT

Magnetic reconnection coupled with nonlinear anisotropic heat conduction is studied by using a two-dimensional magnetohydrodynamic (MHD) simulation. Owing to the heat conduction effect, the adiabatic slow-mode MHD shocks that emanate from the neutral point are dissociated into conduction fronts and isothermal shocks. The dependence on heat conductivity of the physical variables in the outflow region, such as temperature, density, and velocity, are studied. We also discuss the energy release and the reconnection rate.

Subject headings: conduction — MHD — plasmas

1. INTRODUCTION

Magnetic reconnection provides a mechanism for converting magnetic energy to the bulk thermal and kinetic energies of the plasma in a dynamical timescale (e.g., Parker 1963; Sweet 1958; Petschek 1964; Priest & Forbes 1986; Jamitzky & Scholer 1996). Reconnection has been thought to play a fundamental role in the occurrence of flares and jets on the Sun (e.g., Priest 1982; Shibata et al. 1995; Yokoyama & Shibata 1995, 1996), and in the occurrence of substorms in the terrestrial magnetospheres (e.g., Scholer 1989; Birn, Hesse, & Schindler 1996). About the solar flares, several pieces of evidence have been found by the *Yohkoh* observations that are consistent with the magnetic reconnection model (Tsuneta et al. 1992; Masuda et al. 1994; Shibata et al. 1995; Shibata 1996). In particular, Tsuneta (1996) has analyzed the detailed physical conditions in the well-resolved flares and found that they are well explained by reconnection. His work, however, is based on the order-of-magnitude estimate. It is necessary to construct a detailed theoretical model that can be compared directly with the observations.

In this context, there have been many studies on magnetic reconnection, which include various physical effects appropriate for solar flares, such as the line-tying boundary (e.g., Magara et al. 1996), the radiative cooling (Forbes & Malherbe 1991), and so on. However, there are only a few works that studied the heat conduction effect on magnetic reconnection (e.g., Forbes, Malherbe, & Priest 1989; Oreshina & Somov 1996). Edmiston & Kennel (1986) and Kennel (1987) have studied the effect of heat conduction on slow-mode MHD shocks, which could be applied to the fast reconnection model by Petschek (1964). Xu & Forbes (1992) have also extensively studied the structure of slow-mode MHD shocks in a plasma where both heat conduction and radiative cooling are important. In considering hot plasmas, it is important to take into account the heat conduction effect because the timescale of heat conduction is almost comparable to, or very often faster than, that of the flow, i.e., Alfvén timescale. There are two interesting natures of the heat conduction in the hot plasma, although, at the same time, they are the causes of the difficulty for study. One is the nonlinearity: Heat conductivity increases with increasing temperature nonlinearly (e.g., $\propto T^{5/2}$ in collisional plasma). In the magnetic reconnection model of flares, the plasma temperature increases locally near the magnetic neutral point. It will make thermal conductivity nonuniform in space and time. The other is the anisotropy: Heat flux can only conduct along the magnetic field direction (e.g., Priest 1982). This effect would change the structure of the reconnection site and also would change the release rate of the energy.

We developed a numerical magnetohydrodynamic (MHD) code that includes *nonlinear anisotropic* heat conduction (Yokoyama 1995). Using this code, we performed a two-dimensional simulation of the magnetic reconnection coupled with heat conduction.

2. MODELS

The initial condition of the simulation is similar to that of the study by Ugai & Tsuda (1977). It is in magnetohydrostatic equilibrium with antiparallel magnetic fields in the (x, z)-plane (positive x-direction in $z > 0$, and negative in $z < 0$), between which there is a current sheet in $|z| < \delta$. The plasma beta, the ratio of the gas pressure to the magnetic pressure, is taken to be $\beta = 0.03$. The units of length, velocity, and time in the simulations are δ, C_s, and $\tau \equiv \delta/C_s$, respectively, where δ and C_s are the half-thickness of the initial current sheet and the sound speed of the initial condition. We assume that the units of the temperature, the density, and the length are, respectively, $T = 4 \times 10^6$ K, $n_{\rm normal} = 2 \times 10^9$ cm^{-3}, and $\delta = 10^9$ cm. In this initial condition, the temperature is uniform and unity. The density outside the current sheet is taken to be unity. In dimensional units, the sound velocity is $C_s \approx 230$ km s^{-1}, the Alfvén velocity is $V_{\rm A} \approx 1500$ km s^{-1}, and the heat conduction coefficient is $\kappa \equiv \kappa_0 T^{5/2} \approx 3.2 \times 10^{10}$ ergs s^{-1} cm^{-1} K^{-1} for $T = 4 \times 10^6$ K (where $\kappa_0 \approx 10^{-6}$ ergs s^{-1} cm^{-1} K^{-1}), and so the sound-crossing time $\tau \equiv \delta/C_s \approx 43$ s, the Alfvén-crossing time $\tau_{\rm A} \equiv \delta/V_{\rm A} \approx 6.7$ s, and the heat conduction time $\tau_c \equiv \delta^2(n_{\rm normal} k_{\rm B}/\kappa) \approx 8.6$ s, where $k_{\rm B}$ is the Boltzmann constant. Thus, the conduction time is comparable to the Alfvén-crossing time. In order to initiate the magnetic reconnection, we assumed a localized resistivity near the origin $(x, z) = (0, 0)$ as $\eta = \eta_0[2(r/r_\eta)^3 - 3(r/r_\eta)^2 + 1]$ for $r \le r_\eta$, and 0 for $r > r_\eta$, where $r \equiv (x^2 + z^2)^{1/2}$ is the distance from the origin, and $r_\eta = 0.8\delta$ is the size of the region. The magnetic Reynolds number (or, more exactly, the Lundquist number) is $R_m \equiv V_{\rm A} L_{\rm box}/\eta_0 \approx 3600$, where $L_{\rm box} \approx 60\delta$ is the size of the simulation box.

We solved the two-dimensional, nonlinear, time-dependent, resistive, compressible MHD equations. Ohmic heating and heat conduction are taken into account for heat loss and gain.

The conduction coefficient is the Spitzer-type one that is proportional to $T^{5/2}$. We also assume that it is anisotropic, working only in the direction along the magnetic field line so that $\kappa_\parallel = \kappa_0 T^{5/2}$ and $\kappa_\perp = 0$ in the simulations, where $\kappa_\parallel$ and $\kappa_\perp$ are, respectively, the conductivity along and across the magnetic field. (Note that, if we take into account the numerical diffusivity, the conductivity across the field line is *not* zero. The effective value would be estimated as $\kappa_\perp/\kappa_\parallel \ll 0.01$). The specific heat ratio is taken to be $\gamma = 5/3$. In the numerical procedures, the modified Lax-Wendroff method is adopted for the MHD part of the calculations, and the red and black overrelaxation method is adopted for the heat conduction part (e.g., Hirsch 1988). We assumed the symmetry, and only the first quadrant ($0 < x < 70$ and $0 < z < 60$) was calculated. The numerical boundary conditions used for the temperature are zero heat-flux (i.e., $\nabla T = 0$) conditions. They were set far from the region of interest (i.e., $x = 70$ and $z = 60$), thus yielding no significant effect in the present results. Nonuniform grids are used for both x- and z-directions. The number of grid points is 280×240. The minimum grid sizes are $\Delta x = 0.05$ and $\Delta z = 0.02$, which are concentrated near the neutral point. Note that the thinnest part of the current sheet obtained in the simulations has a thickness of 0.2. Thus, our simulations resolved the sheet with at least 10 grid points.

3. RESULTS

The upper panel of Figure 1 (Plate L8) shows the results at $t = 16$ in the case *without* heat conduction. Note that the figure displays only a part ($-5 \le z \le 5$, $0 \le x \le 20$) of the simulation box near the neutral point. Initially, B_x is positive in $z > 0$ and negative in $z < 0$, and there is a current sheet in $|z| < 1$. Reconnection occurs at the origin in this current sheet where localized resistivity is imposed. The reconnected field lines, together with the frozen plasma, are ejected from the neutral point at the origin to the positive and negative x-directions because of the tension force of the reconnected field lines. To complement this outflow, an inflow takes place from positive and negative z-directions of the current sheet. At the boundary between this inflow and the outflow, a *slow-mode MHD shock* is formed, which is predicted by Petschek (1964) in his reconnection theory. Since there are two sets of inflow, from the positive and the negative z-directions, a pair of the shocks is formed, emanating from the neutral point. The close-up plot (upper right panel of Fig. 2 [Pl. L9]) shows a clear jump of the pressure at these shocks. The temperature in the region between these shocks is higher than that outside this region (upper left panel of Fig. 2). This is due to the shock heating.

In the case *with* heat conduction, the apparent distribution of the temperature (lower panel of Fig. 1) is very different from that in the previous case without heat conduction. The high-temperature region is broader than that in the case without heat conduction. The outer boundary of this high-temperature region is a *conduction front*. The conduction front traces the magnetic field line from the neutral point, namely, separatrices. This is due to the following reasons: First, the heat conducts only in the direction along the magnetic field line. Second, the propagation of the conduction front is very fast because the temperature between the conduction fronts is 8 times the initial value, and hence the timescale of the conduction is less than 1/100 times the initial one. Thus, it is about 100 times faster than the Alfvén timescale.

Other than the conduction front, there is a strong jump structure in the pressure distribution (lower right panel in Fig. 2), of which the position is not coincident with that of the conduction front. It is seen that the velocity and the magnetic field change the direction and the amplitude at the same place. Nevertheless, there is no jump in the temperature. Thus, this discontinuous structure is understood as an *isothermal slow-mode MHD shock*.

Figure 4 shows one-dimensional plots of various physical variables at $t = 30$, when the distribution becomes nearly steady state (Fig. 3), and along $x = 20$, which is well upstream of the plasmoid (and the corresponding fast-mode MHD shock) ejected in the positive x-direction. Note that the plots in Figures 3 and 4 are for a much later time ($t = 30$) than for Figures 1 and 2. The thin lines correspond to the results of the case without conduction. The strong jumps at around $z = \pm 1$ are the slow-mode MHD shocks. The thick lines correspond to the results of the case with conduction. It is clearly seen that the high-temperature region is broader in the case with conduction than in the case without conduction (Fig. 4*a*). The boundaries of this hot region around $z = \pm 2.5$ are the heat conduction fronts. Note that the density keeps its value across these fronts (Fig. 4*b*). There is also only weak change in the velocities (Figs. 4*e* and 4*f*). On the other hand, in the pressure distribution, a strong jump structure is seen at $z = \pm 1$ (Fig. 4*c*). The position of this jump is coincident with that of the slow-mode shocks in the case without conduction. The velocity and the magnetic field change the direction and the amplitude at the same place. Since there is no jump in the temperature, this discontinuous structure is an isothermal slow-mode MHD shock. It is interesting to note that the value of the temperature at the symmetrical axis $z = 0$ is somewhat less than that for the case without conduction. This is because heat is transferred by conduction from the high-temperature region (between the shocks) to the outside. Xu & Forbes (1992) derived an analytical solution of the slow-mode MHD shocks coupled with heat conduction effect. They predicted that the magnetic field component B_x should decrease while the velocity component V_x should increase in the upstream of the isothermal slow-mode shock. Our results of B_x in Figure 4*g* support their predictions, although it is not clear whether the results of V_x in Figure 4*e* are consistent with their predictions.

We can interpret this result as follows (Forbes et al. 1989): The plasma that crosses the shocks is heated up because of the shock heating. Thus, a temperature gradient is formed across the shocks. The temperature gradient generates a propagating heat conduction front, and hence the adiabatic slow-mode shock is dissociated into a conduction front and an isothermal slow-mode shock. This will end up in the leakage of the heat because of the conduction across the shocks toward the upflow region. In summary, the effect of the heat conduction is to make the adiabatic slow-mode MHD shocks emanating from the neutral point to be dissociated into conduction fronts and isothermal shocks.

Next, the physical condition of the reconnection outflow region is investigated. Here the dependence of the reconnection outflow region on heat conduction is studied. We studied this by changing the value of the initial density since the conductive cooling time is proportional to the density. Figure 5 shows the physical quantities at $x = 20$ and $z = 0$ at $t = 30$ as functions of density, $n_{\rm normal}$. At this time, the system settles in an approximate steady state, and the values of physical variables at this point do not change in time except for

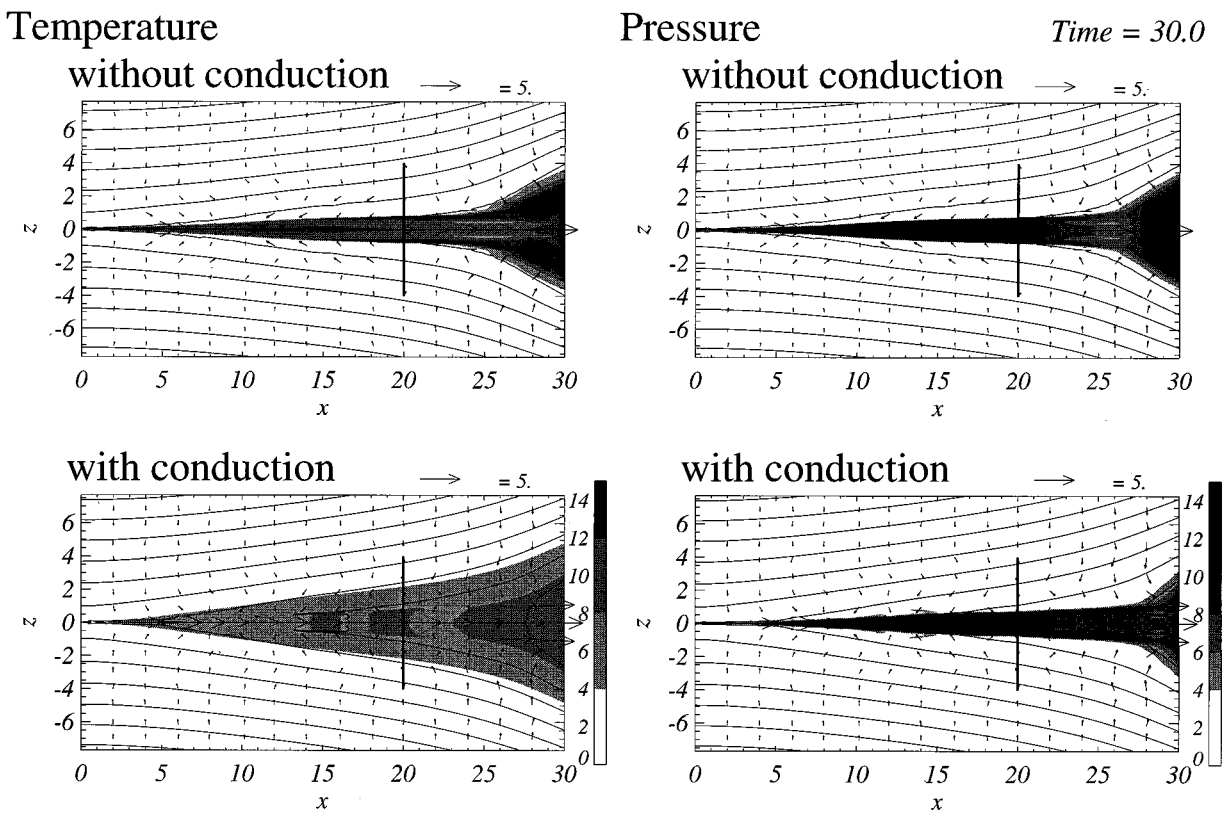


FIG. 3.—Two-dimensional distributions at $t = 30$ of temperature (*left panels*), pressure (*right panels*), magnetic field lines (*solid lines*), and velocity vectors (*arrows*) for the case *without* heat conduction (*upper panel*) and for the case *with* heat conduction (*lower panel*). The levels of the gray-scale map are shown to the right. The unit of velocity vectors is shown at the top right of the figure, whose size is $V = 5.0$ in units of the initial sound velocity. The unit of length is the initial half-thickness of the current sheet. The dimensional units of the length, the temperature, and the density are, respectively, $\delta = 10^9$ cm, $T = 4 \times 10^6$ K, and $n_{\rm normal} = 2 \times 10^9$ cm^{-3}. The initial plasma beta is $\beta = 0.03$, and the Alfvén velocity is $V_A \approx 6.5 \approx 1500$ km s^{-1}. The thick line between $(x, z) = (20, -4)$ and $(20, 4)$ indicates the position along which the one-dimensional plots in Fig. 4 are shown.

oscillations with small amplitude. It is seen that the temperature decreases with decreasing $n_{\rm normal}$ (i.e., with decreasing conductive cooling time $\tau_c \equiv \delta^2(n_{\rm normal}k_B/\kappa)$; Fig. 5*a*). The density increases with decreasing conductive time (Fig. 5*b*). Nevertheless, there are only small changes in pressure, velocity, and magnetic field strength (Figs. 5*c*–5*f*). Thus, owing to the heat conduction effect, the temperature decreases in the downflow region of the reconnection. However, the dynamical structures, such as pressure and velocity, are weakly affected. The dependence of the reconnection rate and the energy release rate on $n_{\rm normal}$ is another interesting issue. Although we changed the value of $n_{\rm normal}$ in 3 orders of magnitude, there is very weak dependence. Thus, we concluded that the reconnection rate is weakly affected by the heat conduction in the present model.

4. DISCUSSION

In the present study, we have studied the effect of heat conduction on magnetic reconnection initiated by the steady localized resistivity. We found that the heat conduction introduces the following effects in the magnetic reconnection: (1) An adiabatic slow shock is dissociated to a conduction front and an isothermal slow shock (as has been predicted by Forbes et al. 1989). (2) In the reconnection jet (i.e., slow shock region), the temperature becomes smaller (about a factor 2), whereas the density becomes larger in the case with conduction rather than in the case without it. (3) The reconnection

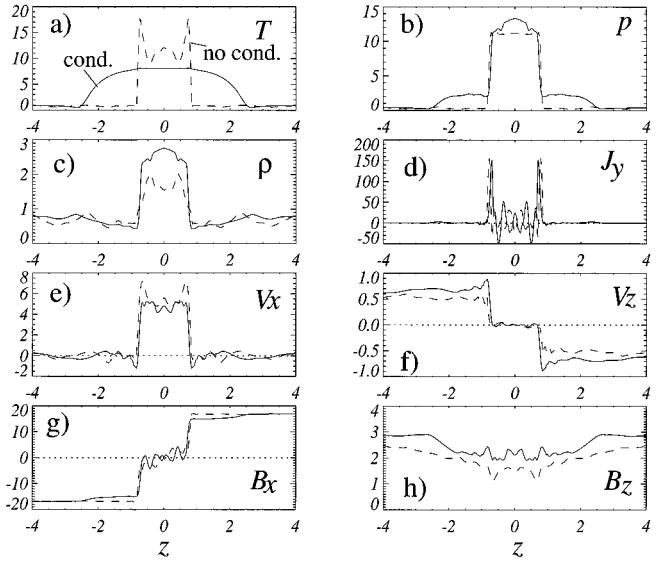


FIG. 4.—One-dimensional distributions of the various physical quantities in z at $x = 20$ across the MHD slow-mode shocks and the heat conduction fronts at $t = 30$. The dashed line corresponds to the case *without* heat conduction. The solid line corresponds to the case *with* heat conduction. The displayed variables are (*a*) the temperature, (*b*) the pressure, (*c*) the density, (*d*) the current density, (*e*) x-component and (*f*) z-component of the velocity, and (*g*) x-component and (*f*) z-component of the magnetic field.

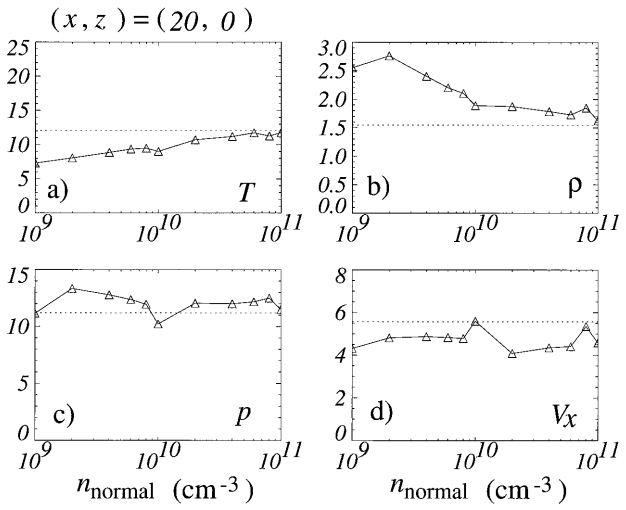


FIG. 5.—The dependence of the physical quantities in the reconnection outflow [at $(x, z) = (20, 0)$; the time is at $t = 30$] on $n_{\rm normal}$ (initial density) in $\rm cm^{-3}$, which is inversely proportional to the thermal conductivity. The displayed variables are (*a*) the temperature, (*b*) the density, (*c*) the pressure, and (*d*) the outflow velocity. The temperature decreases with increasing thermal conductivity. The dashed lines indicates the results of the case without heat conduction.

rate and the energy release rate are weakly affected by heat conduction. (4) As a result of the propagation of the heat conduction fronts, the two-dimensional distribution of hot plasma forms a cusplike shape. Among these effects, the third effect may depend on the resistivity model. In the present study, the resistivity is fixed in space as well as in time. This might give a strong limitation on the structure of the diffusion region near the neutral point. In other resistivity models, e.g., the model in which the magnitude of the resistivity depends on the current density, there is a possibility that this conclusion will be changed. A more detailed study is necessary in order to get a more general conclusion, and the results of such a study will be reported in the near future.

Other than the direct effect on the magnetic reconnection itself, heat conduction also introduces another effect. It is the so-called chromospheric evaporation (Hirayama 1974). The heat energy released around the reconnection site could be conducted along the field lines to the chromosphere. Then a sudden increase of temperature in the upper chromosphere leads to an ablation of chromospheric plasma. This may cause the backflow to the reconnection site to affect the reconnection itself. This effect is also very important. We will discuss this effect in a separate paper.

By our simulation, the distribution of hot plasma forms a cusplike shape. This may give an interesting implication for explaining the cusp-shaped loop structures observed in the long-duration–event (LDE) flares and the large-scale arcade formations in the solar corona (Tsuneta et al. 1992; Tsuneta 1996; Yoshida & Tsuneta 1996; Forbes & Acton 1996; Hanaoka 1994; McAllister et al. 1996; Hiei, Hundhausen, & Sime 1993). Although, in order to make a direct comparison between the observations and the numerical results, we need to take the evaporation effect into account since the observed bright X-ray cusp shape may be formed by the evaporated dense plasma, the formation of the cusp-shape temperature distribution in our simulation may give strong support for the magnetic reconnection as the basic mechanism of these phenomena.

We thank Drs. M. Scholer, T. Terasawa, and F. Jamitzky for fruitful discussions. The computations were done using the supercomputers at the National Astronomical Observatory of Japan.

REFERENCES

Birn, J., Hesse, M., & Schindler, K. 1996, J. Geophys. Res., 101, 12939
Edmiston, J. P., & Kennel, C. F. 1986, J. Geophys. Res., 91, 1361
Forbes, T. G., & Acton, L. W. 1996, ApJ, 459, 330
Forbes, T. G., & Malherbe, J. M. 1991, Sol. Phys., 135, 361
Forbes, T. G., Malherbe, J. M., & Priest, E. R. 1989, Sol. Phys., 120, 258
Hanaoka, Y. 1994, in Proc. Kofu Symp., New Look at the Sun with Emphasis on Advanced Observations of Coronal Dynamics and Flares, ed. S. Enome & T. Hirayama (NRO Rep. 360), 181
Hiei, E., Hundhausen, A. J., & Sime, D. G. 1993, Geophys. Res. Lett., 20, 2785
Hirayama, T. 1974, Sol. Phys., 34, 323
Hirsch, C. 1988, Numerical Computation of Internal and External Flows, Vol. 1 (New York: Wiley)
Jamitzky, F., & Scholer, M. 1996, J. Plasma Phys., in press
Kennel, C. F. 1987, J. Geophys. Res., 92, 13427
Magara, T., Mineshige, S., Yokoyama, T., & Shibata, K. 1996, ApJ, 466, 1054
Masuda, S., Kosugi, T., Hara, T., Tsuneta, S., & Ogawara, Y. 1994, Nature, 371, 495
McAllister, A. H., Dryer, M., McIntosh, P., & Singer, H. 1996, J. Geophys. Res., 101, 13497
Oreshina, A. V., & Somov, B. V. 1996, Astron. Rep., 40, 263
Parker, E. N. 1963, ApJS, 8, 177
Petschek, H. E. 1964, in Proc. AAS-NASA Symp., the Physics of Solar Flares, ed. W. N. Hess (SP-50; Greenbelt: NASA), 425
Priest, E. R. 1982, Solar Magnetohydrodynamics (Dordrecht: Reidel)
Priest, E. R., & Forbes, T. G. 1986, J. Geophys. Res., 91, 5579
Scholer, M. 1989, J. Geophys. Res., 94, 8805
Shibata, K. 1996, Adv. Space Res., 17(4/5), 9
Shibata, K., Masuda, S., Shimojo, M., Hara, H., Yokoyama, T., Tsuneta, S., Kosugi, T., & Ogawara, Y. 1995, ApJ, 451, L83
Sweet, P. A. 1958, in IAU Symp. 6, Electromagnetic Phenomena in Cosmical Physics, ed. B. Lehnert (Cambridge: Cambridge Univ. Press), 123
Tsuneta, S. 1996, ApJ, 456, 840
Tsuneta, S., Hara, H., Shimizu, T., Acton, L. W., Strong, K. T., Hudson, H. S., & Ogawara, Y. 1992, PASJ, 44, L63
Ugai, M., & Tsuda, T. 1977, J. Plasma Phys., 17, 337
Xu, P., & Forbes, T. G. 1992, Sol. Phys., 139, 315
Yokoyama, T. 1995, Ph.D. thesis, Graduate University for Advanced Studies (Natl. Astron. Obs.)
Yokoyama, T., & Shibata, K. 1995, Nature, 375, 42
———. 1996, PASJ, 48, 353
Yoshida, T., & Tsuneta, S. 1996, ApJ, 459, 342

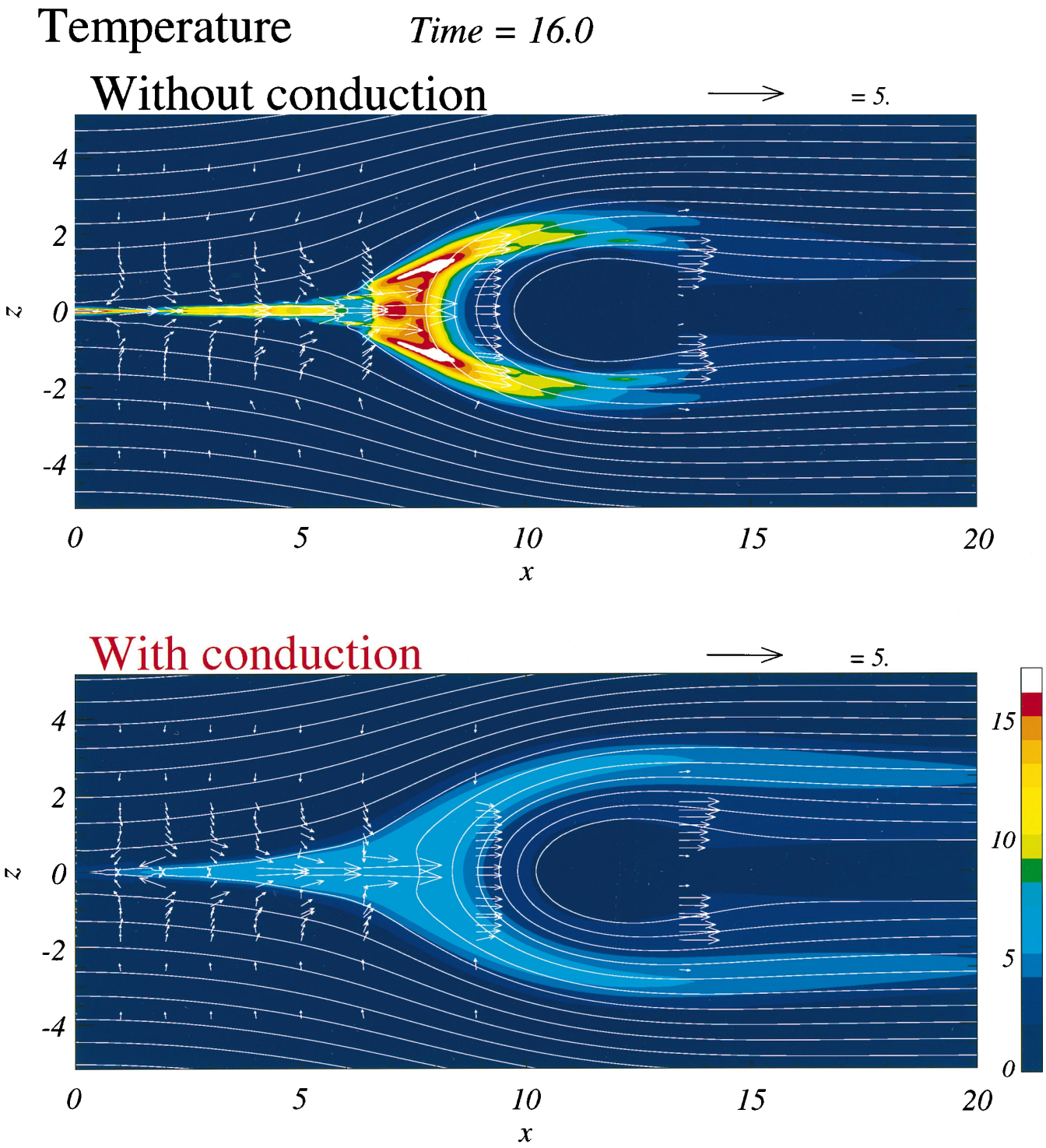


FIG. 1.—Two-dimensional distributions at $t = 16$ of temperature (*color map*), magnetic field lines (*solid lines*), and velocity vectors (*arrows*) for the case *without* heat conduction (*upper panel*) and for the case *with* heat conduction (*lower panel*). The levels of the color map are shown to the right. The unit of velocity vectors is shown at the top right of the figure, whose size is $V = 5.0$ in units of the initial sound velocity. The unit of length is the initial half-thickness of the current sheet. The dimensional units of the length, the temperature, and the density are, respectively, $\delta = 10^9$ cm, $T = 4 \times 10^6$ K, and $n_{\rm normal} = 2 \times 10^9$ cm^{-3}. The initial plasma beta is $\beta = 0.03$, and the Alfvén velocity is $V_{\rm A} \approx 6.5 \approx 1500$ km s^{-1}.

YOKOYAMA & SHIBATA (see 474, L62)

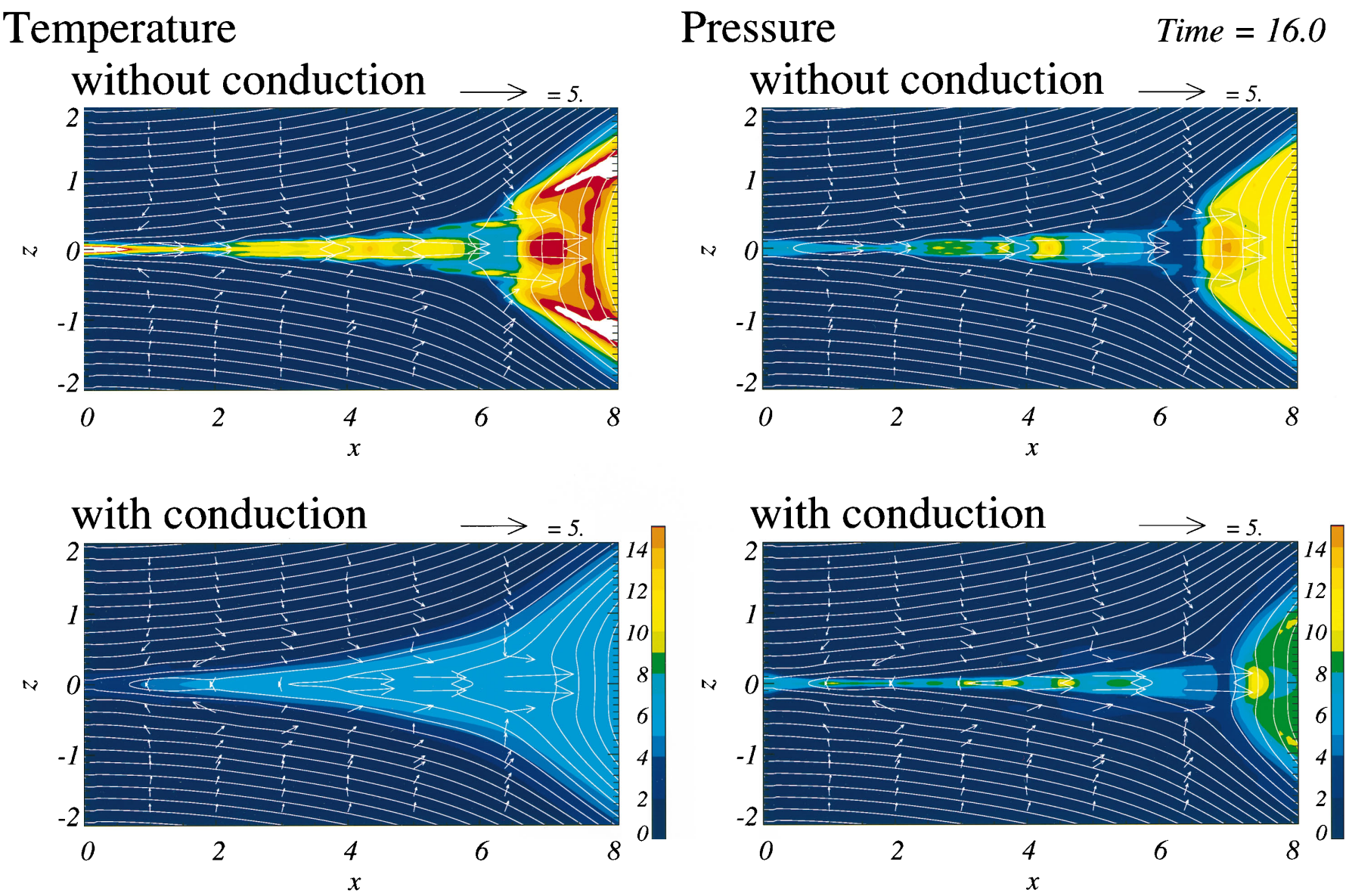


FIG. 2.—Close-up of two-dimensional distributions of the temperature (*left panels*) and the pressure (*right panels*) for the case *without* heat conduction (*upper panels*) and for the case *with* heat conduction (*lower panels*). The others are the same as in Fig. 1.